# The Kinetics and Mechanism of Interaction of $Fe_{40}Ni_{40}B_{20}$ Amorphous Metallic Alloys with Mineral Acid Media

**Adam Košturiak, Ladislav Valko,† Jiří Polavka,*,†† Milan Brutovsky, and Harry Morris†††**

Department of Physical and Analytical Chemistry, Faculty of Natural Sciences, Moyzesova 11, 04154 Košice, Slovak Republic

†Department of Physics, Trenčín University, Študentská 2, 911 50 Trenčín, Slovak Republic

††Department of Physical Chemistry, Faculty of Chemical Technology, Slovak Technical University, Radlinskeho 9, 81237 Bratislava, Slovak Republic

†††School of Pharmacy and Chemistry, Liverpool John Moores University, Liverpool L3 3AF, UK

(Received October 8, 1998)

The paper emphasizes the importance of amorphous metallic alloys thin films for magnetic coatings as well as their characterisation with respect to the mineral acid medium in a more qualitative way. The kinetics and mechanism of the interaction of Fe–Ni–B amorphous alloys films with various concentrations of mineral acids (*o*-phosphoric acid, sulfuric acid, hydrochloric acid, nitric acid,) were studied. On the basis of the weighing method used we deduced that the overall physically and chemically complicated process consists of simultaneous formation of oxides on the surface of the thin films, their dissolution and moreover dissolution of the metal (Fe, Ni) and metalloid (B) elements through a tendency of all of them to react with hydrogen ions. It should be stressed that dissolution of the two-dimensional amorphous metallic alloys-ribbons significantly differs from such dissolution of the metal bulk systems.

Although many problems associated with amorphous metallic alloys (AMAs) are not fully understood, it is already clear that AMAs have mechanical, magnetic, electrical and chemical properties suitable for numerous applications. In additions to the many desirable physical properties, ANAs also appear to have unusual chemical properties such as corrosion resistance which may lead to applications in, for example, a cable that is resistant to sea water and as new biomaterials. In spite of the evident technological importance of the metal-metalloid alloys, our understanding of their physico-chemical behaviour is still at a surprisingly low level. The key to progress seems to be in resolution of their physico-chemical behavior under various conditions. Aqueous corrosion oxidation phenomena of metals have been well studied, but about oxidation of AMAs in the mineral acids little is known. For this reason the investigation of AMAs in the mineral acid media seems both interesting and purposeful. The aim of the present research was to investigate the kinetics and mechanism of interaction between a reactive surface layer of AMA and dilute or concentrated solution of mineral acids resulting in either oxidation of them followed by dissolution or simultaneous oxidation.

Traditional theories of metallic oxidation[1] suppose the formation of an effectively uniform and continuous coating of oxide upon the metal. Exceptions, at least in the initial stages of oxidation, are those metals in which the molar volume of the oxide is less than that of the pure metal. The oxide coating of many metals, however, behaves as though it was continuous, like a film of paint. On the other hand, it appears that the anticorrosion properties of AMAs depend upon the alloying-metallic and amorphising-metalloid elements.[2,3] It has been shown, for example, that the anticorrosion stabilities of the AMAs type $FeMP_{13}C_7$, where M is an alloying element, in aqueous solution of 0.1 M HCl (1 M = 1 mol dm$^{-3}$) at the ambient temperature can be arranged in order of their relative anticorrosion stability as follows: Co < Ni < V < Cr < Ti Cu < Mn. In addition the influence of amorphising elements on the corrosion stability of the AMAs, e.g. $Fe_{70}Cr_{10}B_{13}X_7$ and $Fe_{70}Cr_{10}P_{13}X_7$, where X is B, P, Si, or C, in an aqueous solution of 0.05 M $H_2SO_4$ at 30 °C can also be arranged in order of their anticorrosion stability P < C < B < Si. In the case of $Fe_{40}Ni_{40}B_{20}$ AMAs prepared in the oxygen atmosphere it was found that the rate of adsorption of oxygen on the surface of AMAs which is followed by the creation of an oxide film is much slower in comparison with the Fe-alloys in which Ni was not present.[3] On the other hand it has been well established that various macroscopic chemical properties of the AMAs prepared by the rapid quenching method are dependent to a considerable extent on the physical and chemical state of their surface.[3—6] Unfortunately the time-stability of the desired properties of AMAs appears to be inferior to those of the more classical types of materials, however, coating the AMAs with a thin surface layer of either an organic or an inorganic material simultaneously increases their electroinsulating, anticorrosive and magnetic properties.[7—10]

## Experimental

**Sample Preparation and Measuring Condition.** The amorphous $Fe_{40}Ni_{40}B_{20}$ ribbons used in this experiment were prepared in the Institute of Experimental Physics, Slovak Academy of Sciences, Košice, Slovakia, by the method of extremely rapid quenching of the melt onto a rotating disk. The manufactured ribbons originating from the melting procedure, designated as No. 1 and No. 2, were of 40—60 meters long and were prepared under the following technological conditions: The melting temperature was 1250 °C, working pressure–tension 150 kPa, linear velocity of the cooling disk 24 m $s^{-1}$. The melt was fired under argon pressure against the quartz crucible slit with dimensions 0.4×4 mm. The master analysis was carried out on the AMA ribbon JCX 733 (JEOL, Japan). The chemical composition of the master AMA, and the ribbons prepared from it, were practically the same. The materials were supplied by Johnson Matthey (UK).

The width of ribbons No. 1 was 4.9 mm, whereas that of No. 2 was 5.0 mm; the thickness of both was 42±2 μm. From these ribbons, sections from 1.0 to 5 cm long were cut and subsequently weighed on a semimicrobalance SARTORIUS type 2674 (BRD).

In the present work, two different approaches were employed and mutually compared concerning the estimation of statistical characteristics of the measuring quantities, e.g., the classical mathematical-statistical point estimation approach,[11] and the procedure allowing estimation of all the analysed parameters.[12]

**Weight Measurement.** The thickness of a ribbon is among the first attributes quoted, since the magnetic properties of thin films and other behaviour depend on their thickness. In addition to ribbon thicknesses, other important film attributes such as structure and chemical composition are also important. Measurements of the weight of the ribbon appears, at a first glance, to be an easy and direct way to determine film thickness, $d$. Knowing the ribbon mass $m$, the area $A$, and the film density $\rho$, then

$$d = m/A\rho. \tag{1}$$

This simple method has been often used in laboratories where precision mass balances are more common than interferometers or stylus instruments. Value of $d$ so obtained are imprecise because the ribbon density is not known with certainty; however, to a good approximation, if $A$ is const. and $\rho$ is const., then $d \approx m$ and therefore we have chosen a gravimetric method for the evaluation of the film thickness through weight-changes of the ribbons during mineral acid treatment of sample surface layers.

**The Methodology of the Measurement.** Consider a large two-phase AMA solid–liquid system at a given temperature, both phases being separated by a plane surface of area $A$ in the interface region. The solid will be assumed to be completely rigid with a mass $m$. The solid–liquid system interacts through so-called wetting, including phenomena such adhesion, lubrication, immersion, and flotation. The samples of length 1—5 cm were prepared from the manufactured AMA ribbons; then they were washed in acetone, dried, weighed, and finally fixed in a continuously stirred tank reactor (CSTR) of volume $V = 30$ $cm^3$. The procedure was repeated before every weighing and the appropriate acid of a given concentration was added until the samples were submerged in the thermostatic CSTR at a temperature of 25±0.1 °C. The frequency of stirring was 270±20 rotations $min^{-1}$. After a certain time interval, the ribbon samples were taken out from the CSTR, rinsed with water, then with organic solvent, and finally dried and weighed again. The mineral acids used were 0.33 M $H_3PO_4$, 0.5 M $H_2SO_4$, 0.1 and 1.0 M HCl, then 0.1 and 1.0 M $HNO_3$; the measurements were carried out in atmospheric air.

## Results and Discussion

**Oxidation Kinetics.** In this treatment of a very simple model, we assume a flow of oxygen parallel to the plane of the AMA surface located in the CSTR. The universal response of a metal surface exposed to oxygen either in the atmosphere or in a liquid medium is to oxidize. The oxidation product may be a thin adherent film that protects the underlying metal from further attack or a similar but porous layer that may either be removed from the metal surface of allow the diffusion of oxygen to the metal surface and thus offer no protection. What thickness of oxide will from and at what rate are questions which depend on complex kinetics and microstructure considerations, and not on thermodynamics, although from the standpoint of thermodynamics all of the structural metals exhibit a tendency to oxidize.[13] In order to form the metal oxides at the AMA surface, the following sequential steps are assumed to occur

1) Oxygen is transported from the bulk of the solution via diffusion up to the AMA-solution interface.

2) On reaching the AMA surface, it reacts with the metal atoms Fe, Ni and the metalloid atom B and forms oxides.

The respective mass fluxes corresponding to these two steps can be expressed by

$$J_{\text{diff}} = D(c_0 - c_i)/\delta, \tag{2}$$

$$J = kc_i, \tag{3}$$

where $c_0$ and $c_i$ are the concentrations of oxygen in the bulk of the solution, and at the AMA-solution interface respectively. The quantities $D$ and $k$ represent the diffusion coefficient of oxygen in the adsorbed liquid layer, and the chemical reaction rate constant, respectively. Assuming steady state growth implies that $\delta$ is the effective thickness of the adsorbed liquid layer including the diffusion layer. The oxidation rate of the AMA ribbon sample in oxygen containing liquids is much slower in comparison with that in gaseous oxygen-bearing medium, due to the relatively low solubility of oxygen in liquid.[14]

By assuming a steady state oxidation process implying $J_{\text{diff}} \approx J = J_{\text{ox}}$ the above equations can be solved to give

$$J_{\text{ox}} = kc_0/(1 + \delta k/D). \tag{4}$$

Under steady state conditions $c_0$ is constant, further, in the so-called limit case $D \gg \delta k$, then

$$J_{\text{ox}} \approx kc_0 = k_{\text{ox}}. \tag{5}$$

**Oxidation Reactions.** Most metals react rather slowly with oxygen at ordinary temperature in a dilute solution of a mineral acid. The more active the metal is, the stronger reducing agent it is, and it is therefore preferentially oxidized. Thus for the iron and nickel in contact with oxygen in a mineral acid medium, the oxidation proceeds according to the general reactivity scheme:[14]

$$3Fe(s) + 2O_2(ads) \rightarrow FeO(s) + Fe_2O_3(s) \quad (6)$$

and

$$Ni(s) + 1/2O_2(ads) \rightarrow NiO(s) \quad (7)$$

and finally the metalloid boron oxidizes:

$$2B(s) + 3/2O_2(ads) \rightarrow B_2O_3(s) \quad (8)$$

The theory predicts that these three reactions proceed independently of each other, except insofar as they are both governed by the potential drop at the AMA surface. On the basis of this, resulting rate of the AMA oxidation, then $J_{ox} = J_{ox}(Fe)+J_{ox}(Ni)+J_{ox}(B)$ or

$$J_{ox} = [k_{ox}(Fe) + k_{ox}(Ni) + k_{ox}(B)]c_0 = k_{ox}c_0 = k_{ox}, \quad (9)$$

where $k_{ox}$ is the effective rate constant representing the sum of three rate constants of the diffusion-oxidation processes.

Here, diffusion is assumed to be very rapid through the AMA film, since the bottleneck for growth is the interfacial chemical reactions. Thus the kinetics of oxidation of metals in thin film is the zeroth order. Such a situation results when some factor besides concentration limits the rate of reaction or when the concentrations of reactions are naturally maintained constant, as in our case.

**Dissolution Reactions.** Among the commonest types chemical reaction which take place between a metal and a solution containing ions of mineral acids are deposition, corrosion and dissolution. The driving force for the two simultaneous processes, e.g. oxidation for a given amorphous metal alloy and its dissolution, depends on the free-energy change for oxide formation and its simultaneous dissolution. The dissolution of metals in acid can be regarded as consisting of the processes of formation of ions and discharge of ions at a metal surface. The reaction between oxidized AMA surface layer and the mineral acid is a typical irreversible heterogeneous reaction. This can be expressed by the united heterogeneous reaction scheme:

$$FeO(s) + Fe_2O_3(s) + NiO(s) + 10H_3O^+(aq) \rightarrow Fe^{2+}(aq) + 2Fe^{3+}(aq) + Ni^{2+}(aq) + 15H_2O(l) \quad (10)$$

When as metalloid boron oxide $B_2O_3(s)$ reacts with adsorbed $H_2O(l)$ to form boric acid, the presence of $H_3O^+(aq)$ ions acid medium makes the reaction more rapid, i.e.

$$B_2O_3(s) + 3H_2O(ads) \rightarrow 2H_3BO_3(ads), \quad (11)$$

where $H_2O(ads)$ and $H_3BO_3(ads)$ are present in the adsorbed surface-layer. The adsorbed orthoboric acid $H_3BO_3(ads)$ dissociates[15] as

$$H_3BO_3(ads) \rightarrow H_3BO_3(aq) + 3H_2O(l) \rightarrow 3H_3O^+(aq) + BO^{3-}(aq) \quad (12)$$

It is evident that the $BO_3^{3-}$ anions slow down any crossing of metallic ions into the solution.

On the other hand, for reactive ribbon-metal components such as iron and nickel, the dissolution reactions that occur in the mineral acids are more rapid. In sulfuric acid

$$M(s) + 2H_3O^+(aq) + SO_4^{2-}(aq) \rightarrow M^{2+}(aq) + SO_4^{2-}(aq) + 2H_2O(l) + H_2(g)\uparrow \quad (13)$$

Where M(s) is $Fe^0$ or $Ni^0(s)$. Similarly in nitric acid is expected

$$M(s) + 2H_3O^+(aq) + 2NO_3^-(aq) \rightarrow M^{2+}(aq) + 2NO_3^-(aq) + 2H_2O(l) + H_2(g)\uparrow \quad (14)$$

Since $B^0$ dissolves in the non-oxidizing hydrogenchloride acid:[17]

$$B(s) + 3H_3O^+(aq) + 3Cl^-(aq) \rightarrow B^{3+}(aq) + 3Cl^-(aq) + 3H_2O(l) + 3/2H_2(g)\uparrow \quad (15)$$

It would be expected to dissolve also in the oxidizing sulfuric and nitric acid, too:

$$2B(s) + 6H_3O^+(aq) + 3SO_4^{2-}(aq) \rightarrow 2B^{3+}(aq) + 3SO_4^{2-}(aq) + 6H_2O(l) + 3H_2(g) \quad (16)$$

and

$$2B(s) + 6H_3O^+(aq) + 3NO_3^-(aq) \rightarrow 2B^{3+}(aq) + 3NO_3^-(aq) + 6H_2O(l) + 3H_2(g) \quad (17)$$

On the other hand, as is known, boron is one of the most difficult elements to prepare pure; however, its behavior in interactions with mineral acids seems similar with the behaviors of the metallic elements such as iron and nickel.[16] This conclusion can be supported on the basis of the standard potential values of the oxidation reactions $E^o$ of the elements forming AMA material: $Fe^o \rightarrow Fe^{2+}(aq)+2\ e^-$, $E^o = 0.440$ V, $Ni^o \rightarrow Ni^{2+}(aq)+2\ e^-$, $E^o = 0.230$ V, $B^o \rightarrow B^{3+}(aq)+3\ e^-$, $E^o = 0.730$ V. These $E^o$ values demonstrate the tendency of all the three elements to react with 1 M-$H_3O^+$ ions in a 1 M solution of $Fe^{2+}(aq)$, $Ni^{2+}(aq)$, and $B^{3+}(aq)$ ions at 298 K to form $H_2(g)$ at 1 atom.[16] For the present we simply wish to point out that not all acids yield hydrogen when they react with metals ($Fe^\circ$, $Ni^\circ$) and metalloid ($B^\circ$) and also that an acid may be either a (i) non-oxidizing or an (ii) oxidizing agent. The mechanism and kinetics of *o*-phosphoric acid solution influencing the electrotechnical and magnetic parameters of amorphous alloys was object of study in.[11,17,18]

**Dissolution Kinetics of Ribbons.** As we already mentioned, one of the commonest types of chemical reaction which takes place between an AMA surface layer and a solution containing ions of mineral acid is deposition, corrosion and simultaneous dissolution. All these processes are governed by the complex kinetics. The growth and diminishing kinetics of ribbon of roughly 42 μm thickness described above depends on the several factors associated with the mineral acid–substrate interface, including:

a) Transport of reactants (oxygen and hydronium ion) through the boundary layer to the substrate,

b) Adsorption of reactants at the substrate,

c) Atomic, ion, and molecular surface diffusion, chemical reaction-oxidation, and incorporation into the lattice,

d) Transport of substrate-dissolution away from the substrate through the boundary layer into the mineral acid solution.

To research every individual processes of them and moreover to search every component of the amorphous Fe–Ni–B ribbons, one must use for example, an on-line atomic spectrometer, or the other instruments.

Whenever a material system is not in thermodynamic equilibrium, driving forces arise naturally to push it forward equilibrium. Among such processes one can include the dissolution of solid system. The rate at which these processes take place has been discussed by numerous authors.[19] Nernst established the phenomenological connection between dissolution of material system and diffusion as controlling factor. Applying it to the resultant diffusion transport of molecular species through the two ribbons' interface layers of the magnitude of surface areas $A = 2A'$, one finds that dissolution flow is

$$J_{dis} = dm/Ad\tau = D(m_0 - m)/V\delta \quad (18)$$

and dissolution rate

$$v_{dis} = dm/d\tau = AD(m_0 - m)/V\delta = k_{dis}, \quad (19)$$

where $(m_0 - m)/V\delta$ is the difference mass concentration gradient in a thin ribbon interface surface layer of thickness $\delta$, closely adhered to the amorphous ribbon surface of area $A$, $m/V$ is the mass concentration of the dissolved species in volume $V$ of CSTR at time $\tau$, and $m_0/V$ is the saturated mass–concentration of dissolved species in the interface liquid surface layer in the same volume $V$. If both ribbons' surface areas change smoothly during a dissolution process, we can consider area $A$ as constant and equally $D$, $m_0$, $V$, $\delta$ also constant. Then we can put in Eq. 18 $J_{dis} = k_{dis}$, where $k_{dis}$ is the effective dissolution rate constant at a given temperature. The net weight $m(\tau)$ of the ribbon's sample at time $\tau$ is given by the difference of the flows in Eqs. 9 and 18, e.g. $J_{ox} - J_{dis} = k_{ox} - k_{dis}$, where $k_{dis} > k_{ox}$, or

$$m(\tau) = m_0 - A(k_{dis} - k_{ox})\tau = m_0 - A\kappa\tau \quad (20)$$

where $m_0$ is the initial weight of the sample and $\kappa > 0$ is the effective oxidation–dissolution rate constant. Later $m(\tau)$ will be statistically evaluated. In Fig. 1, two simultaneous processes, e.g. oxidation and dissolution in the mineral acids, in agreement with the Eqs. 6, 7, 8, 9, 10, 11, 12, 13, 14, 15, 16, and 17, are represented. At the amorphous metal–oxygen interface, the neutral metal (Fe, Ni) and metalloid (B) atoms interacting with $H_3O^+$ ions lose electrons and became metal ions. Under the influence of the intensive electric field generated by the anions in solution, these migrate through the metal oxide to the oxygen surface layer into the solution.

The applied steady state condition in which the concentration gradient $(m_0 - m)/V\delta$ is time independent rarely occurs in the case of the dissolution bulk-solids. So the kinetics and mechanism of interaction of the AMAs ribbons as two dimensional system are different from those in the bulk metal system.[20,21]

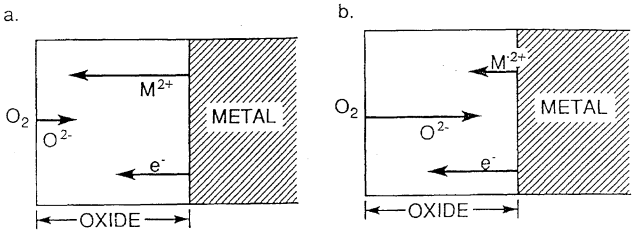


Fig. 1. Mechanisms of oxidation: $M^0 = 2e^- + M^{2+}$; $O_2{}^0 + 2e^- = O_2{}^{2-}$
(a) oxide growth at oxide—ambient interface, (b) oxide growth at oxide—metal interface.

## Comparison with the Experimental Results

**Dissolution Rate and Weight-Loss.** The effect of the stirring rate on the reaction is essentially to change the thickness of the diffusion surface layer. From the dependence of the total dissolution rate on the stirring rate it is concluded that the oxidation process occurring simultaneously with dissolution of ribbon samples at the temperature 25 °C is controlled by the diffusion process. Therefore, before accessing a constant rate stirring regime it was necessary to determine the experimental conditions under which the rate of weight-loss of the AMA sample was constant. The effect of stirring on the dissolution rate is demonstrated in Fig. 2. The rate of the oxidation reaction occurring on the AMA surface is slow, e.g. in the case of $H_2SO_4$ acid. In contrast, for example, in the case of 1.0 or 0.1 M-$HNO_3$ acid solution, the dependence dissolution stirring rate is smooth. Statistically evaluated data describing weight-loss of the AMA sample in 0.5 M-$H_2SO_4$ are summarized in Table 1 and losses in 0.1 M-$HNO_3$ in Table 2 and Fig. 3. The data fit a linear time dependence and this fit confirms our theoretical view on the problem, represented by Eq. 20. The statistical parameters characterising the accuracy of measurements in various mineral acids are shown in Table 3. The weight–time dependence decrease of the sample om 0.5 M-$H_2SO_4$ is relatively small and the obtained value of the dissolution rate, $v_{dis} = 4.1 \times 10^{-2}$ mg $min^{-1}$, confirms the slow course of the dissolution proc-

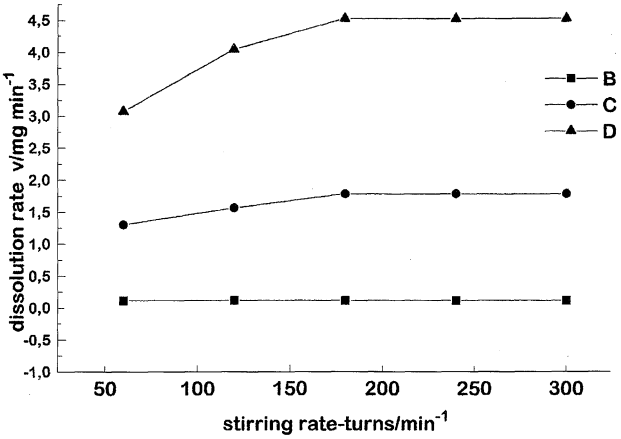


Fig. 2. The dissolution rate $v_{dis}$ vs. stirring rate-turns for the some samples of amorphous $Fe_{40}Ni_{40}B_{20}$ alloys (B : 0.5 M-$H_2SO_4$, C : 0.1 M-$HNO_3$, D : 1.0 M-$HNO_3$).

Table 1. The Statistical Parameters Characterising the Weight-Loss vs. Time in 0.5 M-$H_2SO_4$ for the Amorphous $Fe_{40}Ni_{40}B_{20}$ Alloys ($A = 4.9$ cm$^2$, $t = 25$ °C, Melting No. 1)

| $\tau$/min | $m$ (meas)/mg | $m$ (calc)/mg | $s$% (meas) | $s$% (calc) | $d$% (meas) | $d$% (calc) |
|---|---|---|---|---|---|---|
| 0 | 53.07 | 53.22 | 0.30 | 0.36 | 0.29 | 0.45 |
| 5 | 52.81 | 53.01 | 0.40 | 0.36 | 0.40 | 0.45 |
| 15 | 52.04 | 52.61 | 0.95 | 0.36 | 1.01 | 0.46 |
| 35 | 52.12 | 51.79 | 1.44 | 0.36 | 0.63 | 0.46 |
| 65 | 50.53 | 50.56 | 1.39 | 0.37 | 0.06 | 0.47 |
| 95 | 48.82 | 49.32 | 1.79 | 0.37 | 1.03 | 0.47 |

The number of samples for each set $N = 3$, $\tau$ is time, $m$ (meas) is the measured weight, $m$ (calc) is the calculated weight by the least square method, $s$% (meas) is the point estimate from the relative value of the standard deviation of individual measurements, $s$% (calc) is the functional estimate of the relative value of the standard deviation of individual measurements, $d$% (meas) is the point estimate of the relative error value, $d$% (calc) is the functional estimate of the relative error value, $A$ is the surface area.

Table 2. The Statistical Parameters Characterising the Weight-Loss vs. Time in 0.1 M-$HNO_3$ for the Amorphous $Fe_{40}Ni_{40}B_{20}$ Alloys ($A = 4.9$ cm$^2$, $t = 25$ °C, Melting No. 1)

| $\tau$/min | $m$ (meas)/mg | $m$ (calc)/mg | $s$% (meas) | $s$% (calc) | $d$% (meas) | $d$% (calc) |
|---|---|---|---|---|---|---|
| 0 | 53.42 | 53.26 | 0.02 | 0.41 | 0.30 | 0.92 |
| 5 | 45.13 | 44.46 | 0.60 | 0.81 | 1.49 | 1.02 |
| 10 | 35.46 | 35.66 | 0.13 | 0.91 | 0.56 | 1.15 |
| 15 | 25.11 | 26.86 | 0.51 | 1.04 | 2.95 | 1.31 |
| 20 | 17.39 | 18.06 | 3.44 | 1.26 | 3.71 | 1.59 |
| 25 | 8.92 | 9.26 | 0.88 | 1.73 | 3.67 | 2.19 |
| 30 | 4.75 | 0.46 | 3.48 | 8.69 | 2.61 | 10.98 |

The number of samples for each set $N = 3$. The meaning of the symbols is the same as in the Table 1.

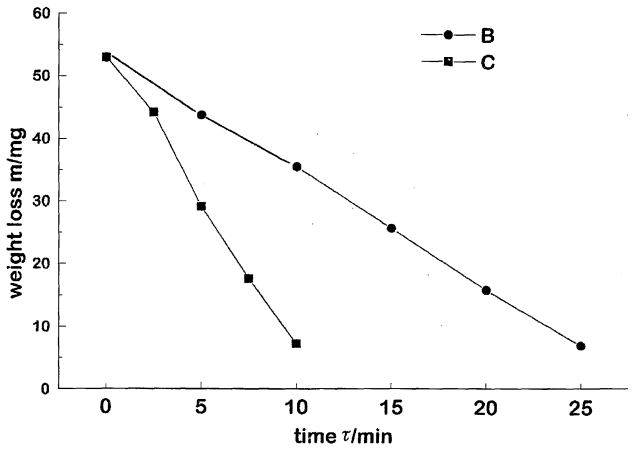


Fig. 3. The weight-loss $m$ vs. time $\tau$ for the some samples of amorphous $Fe_{40}Ni_{40}B_{20}$ (B : 0.1 M-$HNO_3$, C : 1 M-$HNO_3$).

ess. Tables 1, 2, and 3 list the errors in experimental data determined by the liner regression analysis. We can conclude that it is useless to reduce random errors with uncalibrated or inaccurate equipment. However, from the date summarised in Table 2 it follows that in the case of 0.1 M-$HNO_3$ the dissolution weight loss is much higher, even though the concentration of $H_3O^+$ ions is 10-times lower, in comparison with the effect of $H_2SO_4$ acid. The corresponding dissolution rate $v_{dis} = 1.76$ mg min$^{-1}$ (Table 3), but it was found that weight decreases linearly only up to a time of roughly ca. 25 min. Similar data were obtained also in the case of 1.0 M-$HNO_3$ $v_{dis} = 4.62$ mg min$^{-1}$ is higher in comparison with the dissolution rate corresponding to 0.5 M-$H_2SO_4$ at the same experimental measurement conditions. The lowest dissolution rate is observed in the case of 0.1 M-HCl and the rate is little higher in 1.0 M-HCl.

Table 3. The Statistical Parameters Characterising the Liner Time Dependence of the Dissolution Rate $v_{dis}$ in Various Mineral Acids for Amorphous-$Fe_{40}Ni_{40}B_{20}$ ($A = 4.9$ cm$^2$, $t = 25$ °C, Melting No. 1)

| Medium | $N$ | $v_{dis}$/mg min$^{-1}$ | $s_v$ | $a$ | $s_a$ | $\Sigma\Delta^2$ | $r$ |
|---|---|---|---|---|---|---|---|
| 0.5 M-$H_2SO_4$ | 18 | 0.041 | 0.001 | 53.22 | 0.080 | 0.6361 | 0.9900 |
| 0.33 M-$H_3PO_4$ | 18 | 0.040 | 0.001 | 53.28 | 0.034 | 0.1572 | 0.9941 |
| 1.0 M-HCl | 21 | 0.018 | 0.001 | 53.24 | 0.027 | 0.0720 | 0.9825 |
| 0.1 M-HCl | 18 | 0.008 | 0.001 | 53.22 | 0.034 | 0.0963 | 0.9493 |
| 0.1 M-$HNO_3$ | 18 | 1.76 | 0.01 | 53.26 | 0.23 | 1.4529 | 0.9995 |
| 1.0 M-$HNO_3$ | 15 | 4.62 | 0.02 | 53.03 | 0.15 | 1.3689 | 0.9999 |

$N$ is the total number of measurements taken for the calculation, $v_{dis}$ is the dissolution rate, $s_v$-intercept decisive deviation of $v_{dis}$, $a$ is the intercept, $s_a$ is the intercept decisive deviation, $\Sigma\Delta^2$ is the sum of the squared deviations between the measured and by the least squares method calculated values of weight $m$, $r$ is the correlation coefficient.

**The Rate Constants and the Surface Area of Ribbons.** Dependence of dissolution rate $v_{dis}$ on the magnitude of surface area $A$ in the case of 1.0 M-$HNO_3$ is summarised in Table 4, where all data are statistically evaluated. It is remarkable that the dissolution rate at a given temperature and stirring rate decreases with the decreasing surface area of the ribbon samples from 4.72 to 0.92 mg min$^{-1}$. From the analysis of the relationship between the weight-loss of samples versus time dissolution in 1 M-$HNO_3$, it has been found that the extrapolated time interval corresponding to the zero weight sample ($m \approx 0$) tends to ca. 11.5 min, which can be considered as the overall dissolution time (Fig. 3). We can conclude that this extrapolated time interval reasonably correlates with the residuals, e.g. the differences between observed and calculated sample-weight (Table 4). On the other hand, for the purpose of illustration, the dissolution time for the set of ribbon samples weights lying in the interval; 1—6 mg, corresponds roughly to 15 min dissolution time. From this we can conclude that, if more that 85 wt% of the sample is dissolved, the oxidation–dissolution reactions proceed with great velocity (Fig. 4). It is evident that the overall rate of dissolution in general depends not only on the concentration of the mineral acid, but also on the concentration of all the ions present in the solution (Eqs. 19 and 20).

We mention, that the various weighings were accurate to four decimal places and were realised to a level of precision that clearly differentiates one ribbon sample from another. In addition it can be seen that the error in the weight-loss measurements is sufficiently small in comparison with a variation in ribbon sample weight. Statistically evaluated dissolution rate $v_{dis}$ as a function of the ribbon surface area $A$ is represented by the linear Eq. 19 (Fig. 5):

$$v_{dis}/\text{mg min}^{-1} = (0.0120 \pm 0.0021) + (0.9427 \pm 0.0064)A$$
$$N = 15, u = 5, r = 0.9997, \Sigma\Delta^2 = 0.0162, \quad (21)$$
$$A = (1.0 - 5.0)\ \text{cm}^2.$$

From the high value of the correlation coefficient, $r$ it can be concluded that the dissolution rate $v_{dis}$ as a function of surface area $A$ is linear, in harmony with Eq. 19. The calculated values of $v_{dis}$ as well as all the statistical parameters in Table 4 support this conclusion.

However, we can state that, at constant temperature and stirring rate, the dissolution flow $J_{dis}$ is not constant, but apparently decreases with increasing surface area (Tables 3 and 4). This has all the appearances of an edge effect, possibly due to an unequal distribution of ribbon surface inhomogeneities, such as the small pits. This effects is more predominant for smaller areas than for larger ones, thus accounting, at least qualitatively, for the apparently greater rate of dissolution of the smaller surfaces. For this reason it is recommended that in future experiments a complete determination of the rate constants as a function of stirring rate should be carried out for each sample.

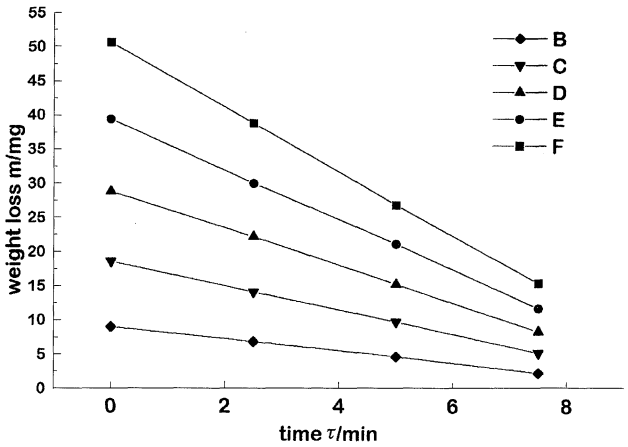


Fig. 4. The weight-loss $m$ vs. time $\tau$ for the some samples of amorphous $Fe_{40}Ni_{40}B_{20}$ in 1 M-$HNO_3$. Area (B) 1 cm$^2$, (C) 2 cm$^2$, (D) 3 cm$^2$, (E) 4 cm$^2$, (F) 5 cm$^2$.

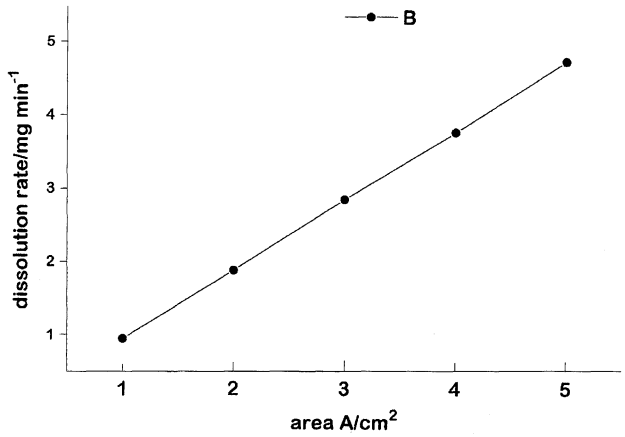


Fig. 5. The dissolution rate $v_{dis}$ vs. the ribbon surface area $A$ of the amorphous $Fe_{40}Ni_{40}B_{20}$ alloys in 1 M-$HNO_3$.

Table 4. The Statistical Parameters Characterising the Dependence of the Dissolution Rate $v_{dis}$ on the Surface Area $v_{dis} = f(A)$ for the Amorphous-$Fe_{40}Ni_{40}B_{20}$ Alloys in 1.0 M-$HNO_3$ ($t$ = 25 °C), Melting No. 2)

| $A$/cm$^2$ | $v_{dis}$/mg min$^{-1}$ | $s_v$ | $a$ | $s_a$ | $\Sigma\Delta^2$ | $r$ | $\tau$ ($m \rightarrow 0$)/min |
|---|---|---|---|---|---|---|---|
| 1.0 | 0.917 | 0.04 | 9.65 | 0.24 | 3.030 | 0.9943 | 9.81 |
| 2.0 | 1.881 | 0.06 | 18.71 | 0.62 | 7.656 | 0.9944 | 10.81 |
| 3.0 | 2.820 | 0.11 | 29.09 | 0.65 | 21.767 | 0.9931 | 10.36 |
| 4.0 | 3.772 | 0.13 | 39.61 | 0.61 | 34.147 | 0.9940 | 10.61 |
| 5.0 | 4.723 | 0.12 | 50.88 | 0.80 | 34.375 | 0.9972 | 10.73 |

$\tau$ ($m \rightarrow 0$) is the extrapolated value of time for dissolution rate of the whole sample, the meaning of the other symbols is the same as in the Table 3.

## Conclusions

Here we present the influence of a mineral acid medium on the $Fe_{40}Ni_{40}B_{20}$ ribbon surface. Our important conclusion is that the kinetics and mechanism of interaction of the amorphous ribbons as a two-dimensional system differs in comparison with the bulk metal system. This interaction is manifested through series of complicated physical and chemical processes. The dominant ones are oxidation processes, represented by the set of reactions, Eqs. 6, 7, and 8, and the dissolution reactions—the Eqs. 10, 11, 12, 13, 14, 15, 16, and 17, which occur simultaneously and both are controlled by the diffusion process. We have not considered reducing reactions since these to be hardly carried out, taking into account the relatively lower solubility of hydrogen in liquid and neglecting its partial hydrogen pressure under the high frequency of stirring in comparison with the favourable component of oxygen. We suppose that oxidizing of the AMA ribbons has two principal advantages: (a) by adjusting the composition of the oxidation products on the surface layer, one can also improve the magnetic characteristics, and (b) an optimally chosen oxide layer on AMA ribbon surface can improve the chemical stability of the AMA and hence stability of their magnetic properties. Comprehensively speaking, a knowledge of the reaction mechanism and influence of mineral acid media on the AMA will enable us to choose accelerating or inhibition conditions for optimisation of oxidation processes and thus influence their magnetic characteristics, too. In addition to the many desirable physical properties of AMA glasses, unusual chemical properties such as corrosion resistance sometimes appear which by the influence of mineral acid medium could be improved. This paper together with many unanswered questions about the chemistry and physics of AMAs promises a stimulating forthcoming work on the subject.

This work has been supported by grant No.1/4208/97 to P. Šimon from the Slovak Grant agency for Science.

## References

1 A. I. Manochin, B. S. Mitin, V. A. Vasiljev, and V. A. Rovjachion, "Amorfnyje Splavy," Izd. Metallurgia, Moskva (1984), p. 104.

2 V. V. Nemoškalenko et al., "Amorfnyje Metalliceskije Splavy," Izd. Naukova dumka, Kijev (1987), p. 197.

3 I. M. Devine, *J. Elektrochem. Soc.*, **38**, 124 (1977).

4 B. S. Mitin and V. A. Vasilev, "Bystrozakalennyje Metally,", Metalluragia, Moskva (1982), p. 424.

5 M. Naka, K. Hashimoto, and T. Masumato, *J. Non-Cryst. Solids*, **30**, 29 (1978).

6 T. I. Bratys, M. A. Vasiljev, and V. T. Ceranin, *Metallofiz.*, **6**, 77 (1984).

7 A. Zentko, A. Košturiak, and P. Duhaj, *IEEE Trans. Magn.*, **20**, 1326 (1984).

8 A. Košturiak, L. Potocký, R. Mlynek, J. Gajdušek, A. Lovas, É. Kissdi-Koszó, and L. F. Kiss, *JMMM*, **4**, 105 (1984).

9 Y. Okazaki, H. Kanno, S. Kousaka, and E. Sakuma, *IEEE Trans. Magn.*, **23**, 3515 (1987).

10 V. Okazaki, H. Kanno, and E. Sakuma, *IEEE Trans. Magn.*, **25**, 3352 (1989).

11 A. Košturiak and O. Duša, *IEEE Trans. Magn.*, **30**, 527 (1994).

12 A. Košturiak and G. Petraš, *Radioaktiv. a živ. prostr.*, **10**, 249 (1987).

13 M. Ohring, "The Materials Science of Thin Films," Academic Press Inc., Harcourt Brace Jovanovich, Publischers, Boston, San Diego, New York, and London (1992).

14 T. B. Grimsley, "Oxidation of Metals in Chemistry of the Solid State," ed by W. E. Garner, Butterworths Scientific Publications, London (1955).

15 A. Košturiak, O. Duša, and J. Gajdušek, *JMMM*, **109**, 27 (1992).

16 J. V. Quagliano, "Chemistry," Prentice-Hall, Inc., Englewood Cliffs, New Jersy (1963).

17 A. Košturiak, L. Valko, J. Polavka, and F. Vasilco, *J. Elect. Eng.*, **48**, 67 (1997).

18 A. Košturiak and L. Valko, *Surf. Coat. Technol.*, **90**, 185 (1997).

19 A. Nernst and P. Brunner, *Z. Phys.*, **47**, 52 (1904).

20 W. J. Moore, *J. Chem. Phys.*, **19**, 255 (1951).

21 G. E. Kimball, *J. Chem. Phys.*, **8**, 199 (1940).